EUROPEAN MECHANICAL SCIENCE

Research Article

e-ISSN: 2587-1110

Data-driven optimization of MIG welding: A synergistic approach for superior joint quality

Raviram R[1*], Ranjith Raj A[1], Shashang G[1], Shameer Mohamed S[1]

[1]Department of Mechanical Engineering, Sri Venkateswara College of Engineering, Sriperumbudur, Tamil Nadu, India

Abstract: A data-driven approach was applied in this research to determine input parameters for producing high-quality welds in mild steel sheets. By utilizing an L16 orthogonal array, the signal-to-noise (S/N) ratio and analysis of variance (ANOVA) techniques were used to optimize weld characteristics. The Multi-Objective Optimization based on Ratio Analysis (MOORA) method was used to rank these conflicting objectives according to their importance in different scenarios. From principal component analysis (PCA), setting the voltage at 42V, welding current at 250A, wire feed rate at 8 mm/min, and gas flow rate at 15 L/min results in ideal characteristics: penetration of 2.961 mm, reinforcement of 5.658 mm, bead width of 12.753 mm, and dilution percentage of 4.183%. Through the MOORA method, it was determined that a voltage of 40V, welding current of 175A, wire feed rate of 4 mm/min, and gas flow rate of 10 L/min would yield optimal weld bead geometry with penetration of 0.884 mm, reinforcement of 6.489 mm, bead width of 11.715 mm, and dilution percentage of 1.218%. This study effectively optimized welding parameters for superior welding in sheet metal fabrication for small and medium-sized enterprises.

Keywords: MIG, Taguchi method, MOORA method, PCA, analysis of variance, optimization

1. Introduction

Many small-scale and medium-scale industries utilize Metal Inert Gas (MIG) welding to manufacture sheet metal components. However, there is a need to utilize the design of experiments to identify the optimum process parameters for improved welding. In MIG welding, heat is applied to fuse a consumable electrode and the base plate metal, which then solidify together to form a robust joint. Mild steel is a readily accessible material, reasonably priced, and finds extensive use in numerous engineering applications [1]. This welding technique offers numerous benefits, including reasonable production speed, optimal cost of the product, strength, and improved surface quality [2,3]. The Metal Inert Gas (MIG) welding process is also referred to by way of Gas Metal Arc Welding (GMAW) [3]. In this procedure, metallic components are melted through the application of heat by an electric arc, while utilizing a consumable wire electrode. The welding gun consistently feeds the filler wire into the weld pool, facilitating the joining of the main materials [4]. A shielding atmosphere, comprising carbon dioxide gas, is established in the working area to safeguard the weld deposit from contaminants [5].

Hot-rolled mild steel has been utilized as the base metal for this study. This material finds use in structural components, railways, agricultural equipment, and various components in machinery and equipment. The voltage, current, wire filler rate, and gas flow rate have important effects on weld joints [6-9].

2. Experiment and Methods

The MIG welding process utilized a Toshweld MIG 400IJ DC inverter source (±2A current stability) and an IGBT Module wire feeder. The gas cylinder was fitted with a gas flow meter (±0.1 L/min). For the experiment, mild steel sheet metal (IS 2062 GR E250) of 2 mm thickness was cut to the desired dimensions of 28×150mm using a punching machine. Plate surfaces were cleaned using wire brushes and emery paper to eliminate any rust. A single bead was then applied to two clean plates using 1.2 mm diameter copper-coated mild steel wire (ER70S-6) while maintaining a pure carbon dioxide gas flow rate and positive electrode polarity to form a butt joint. The chemical compositions of the base material are detailed in ▶**Table 1**, while those of the wire can be found in ▶**Table 2**. All experimental analyses were conducted utilizing Minitab software (version 21.4.2) (RRID:SCR_014483). ▶**Figure 1** illustrates the weld bead geometry.

*Corresponding author:
Email: raviram14082002@gmail.com

Cite this article as:
Raviram, R., *et.al.* (2025). Data-driven optimization of MIG welding: A synergistic approach for superior joint quality. *European Mechanical Science*, 9(2): 103-113. https://doi.org/10.26701/ems.1621888

History dates:
Received: 01.02.2025, **Revision Request**: 03.03.2025, **Last Revision Received**: 18.03.2025, **Accepted**: 07.04.2025

Table 1. Chemical composition of E250

C	Mn	Si	P	S
0.2	1.5	0.04	0.04	0.04

Table 2. Chemical composition of ER70S-6

C	Mn	Si	P	S	Ni	Cr	Mo	V	Cu
0.08	1.625	0.975	0.009	0.035	0.15	0.15	0.15	0.03	0.5

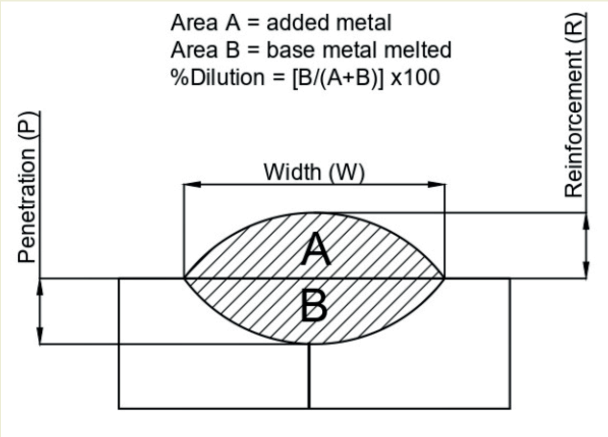

Figure 1. Weld bead geometry

2.1. Selection of process parameters

In order to establish the extent of the input variables, experimental welds were conducted. The key characteristics analyzed for this study include voltage, welding current, gas flow rate, and wire feed speed [6-9]. ▶Table 3 presents the specific input variables by their corresponding levels.

Table 3. Levels of process parameters

Parameters	Level 1	Level 2	Level 3	Level 4
Voltage V, V	40	42	44	46
Current I, A	175	200	225	250
Wire feed rate S, mm/min	4	6	8	10
Gas flow rate G, lpm	10	15	20	25

2.2. Orthogonal array and recording of data

Table 4 presents data showing that sixteen experiments in total were carried out using an L16 orthogonal array. These experiments were carried out randomly to avoid any potential inaccuracies associated with a systematic testing approach [10]. Following the completion of the welding process, cross-sections from the optimal section, typically the middle, of each welded sample were obtained. The weld beads were subsequently analyzed with an Epson L3150 image scanner (5760 × 1440 dpi resolution), which was used to capture individual measurements from the scans. ImageJ software (1:54i03 version) was utilized to determine the dilution percentage by examining the melted areas of both the base material and the material utilized for weld bead height. Detailed results are presented in ▶Table 4, while ▶Figure 2 illustrates the weld bead specimens.

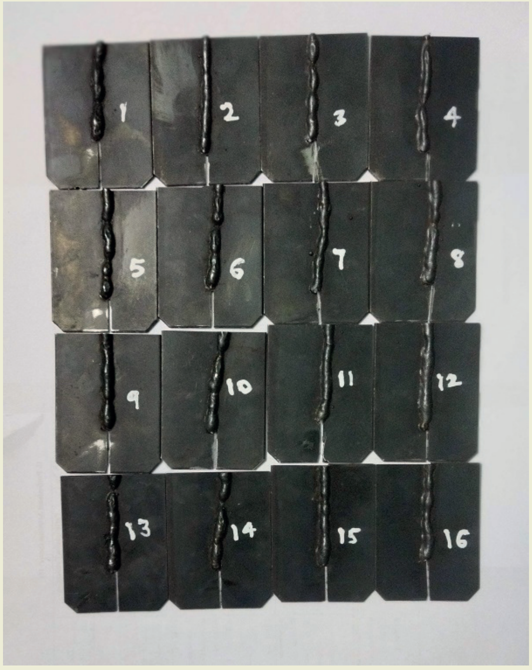

Figure 2. Welded specimens

2.3. Taguchi Method

The Taguchi technique is an effective tool designed for solving issues that can significantly reduce the cost and duration of experiments while improving the performance of the system, layout, procedure, and product [11]. This approach, which blends the concepts of quality loss function and experimental design theory, has been used in the manufacturing sector to solve a number of challenging issues and carry out reliable process and product design. Additionally, this method identifies the characteristics that have the greatest impact on the total performance.

The Taguchi approach yields optimal parameters for the process that are not affected by variations in the surrounding conditions or other noise elements [12]. As the process variables rise, so does the number of experiments. The Taguchi technique uses an orthogonal array arrangement for analyzing the complete process parameters with a restricted number of experiments in order to overcome this complexity. For evaluating quality attributes, S/N ratio is utilized in Taguchi method. The mean (or desired value) of the output characteristics, is represented by the phrase "signal," and the unwanted value, or the square of the deviation, is represented by the term "noise." Consequently, the ratio of mean to the square of the deviation is known as the S/N ratio [13–18]. In the examination of the (Signal/Noise) ratio, Taguchi establishes three categories of quality characteristics, i.e. the lower-the-better, the larg-

 https://doi.org/10.26701/ems.1621888

Table 4. Layout of L16 orthogonal array with experiment values

No.	V	I	S	G	Penetration, mm	Reinforcement, mm	Bead Width, mm	Dilution Percentage
1	40	175	4	10	0.884	6.489	11.715	1.218
2	40	200	6	15	0.775	5.117	9.38	1.292
3	40	225	8	20	0.548	4.173	7.373	1.254
4	40	250	10	25	1.04	3.405	13.023	2.659
5	42	175	6	20	1.733	6.879	11.058	2.092
6	42	200	4	25	1.25	6.127	13.9	1.716
7	42	225	10	10	1.491	5.529	13.046	2.245
8	42	250	8	15	2.961	5.658	12.753	4.183
9	44	175	8	25	1.767	7.124	13.831	2.103
10	44	200	10	20	1.096	7.258	14.023	1.265
11	44	225	4	15	1.386	5.397	15.471	2.175
12	44	250	6	10	1.47	4.956	15.96	2.499
13	46	175	10	15	1.25	7.858	16.681	1.343
14	46	200	8	10	1.491	9.316	16.117	1.345
15	46	225	6	25	2.08	5.768	12.661	2.928
16	46	250	4	20	2.108	5.046	12.479	3.444

er-the-better, and the nominal-the-better. The optimal bead geometry requires smaller the better characteristics for depth of penetration and dilution, while larger the better characteristics for bead width and reinforcement are crucial for optimal design.

The S/N ratio is expressed as follows:

Nominal-the-best,

$$S/N = -10log\, y_i{}^{-2}/s^2 \quad (1)$$

Smaller-the-better,

$$S/N = -10log(\frac{1}{n}\sum_{i=1}^{n} y_i{}^2) \quad (2)$$

Larger-the-better,

$$S/N = -10log(\frac{1}{n}\sum_{i=1}^{n} 1/y_i{}^2) \quad (3)$$

From a sequence of n simulated trials, y_i is the result of the i^{th} trial.

2.4. MOORA method

A method of concurrently improving two or more competing attributes while conforming to specific limitations is called multi-objective optimization [19]. One such multi-objective optimization strategy is the MOORA method, which Brauers first presented [20]. It is a useful tool for resolving a wide range of complicated decision-making problems related to manufacturing settings [19]. The decision matrix that displays the performance of the various alternatives in relation to different characteristics is the primary step when using MOORA method [21–27].

$$X = \begin{bmatrix} X_{11} & X_{12} & \dots & \dots & \dots & \dots & X_{1q} \\ X_{21} & X_{22} & \dots & \dots & \dots & \dots & X_{2q} \\ \dots & \dots & \dots & \dots & \dots & \dots & \dots \\ \dots & \dots & \dots & \dots & \dots & \dots & \dots \\ X_{p1} & X_{p2} & \dots & \dots & \dots & \dots & X_{pq} \end{bmatrix} \quad (4)$$

Where p is the number of alternatives, q is the number of attributes, and X_{ij} is the performance measure of the i^{th} alternative on the j^{th} attribute [19]. Next, a ratio arrangement is developed where the performance of each alternative on an attribute is compared with a denominator that represents all the different alternatives on that attribute. According to the findings of Brauers et al. [21], the most favorable option for this denominator involves calculating the square of the total squared values for each attribute. The resulting is an equation for this ratio:

$$\overset{a}{X}_{ij} = X_{ij}/\sqrt{\textstyle\sum_{i=1}^{m} X_{ij}^2}(j = 1,2, \dots, n) \quad (5)$$

Here X_{ij} represents a dimensionless number which indicates the normalized performance of the i^{th} alternative on the j^{th} attribute and lies inside the interval [0, 1] [19]. These normalized performances are included for multi-objective optimization while maximizing helpful qualities and removed when minimizing non-beneficial attributes. The optimizing problem now changes to

$$Y_i = \sum_{j=1}^{g} \overset{a}{X}_{ij} - \sum_{j=g+1}^{n} \overset{a}{X}_{ij} \quad (6)$$

Where Y_i is the normalized value of the i^{th} alternative with regard to every attribute, g is the number of qualities to be maximized, and (n−g) is the number of qualities to be minimized. It is often observed that certain

https://doi.org/10.26701/ems.1621888

characteristics are more important than others in certain circumstances. A property is multiplied by its corresponding weight to increase its importance [8]. Considering attribute weights to be taken into account, Eq. (6) is modified as follows:

$$Y_i = \sum_{j=1}^{g} W_j \cdot \overset{a}{X}_{ij} - \sum_{j=g+1}^{n} W_j \cdot \overset{a}{X}_{ij} (j = 1,2,\dots,n) \quad (7)$$

Where W_j is the weight of the j^{th} attribute, which is calculated by applying the entropy method. Based on the total of the maximum and minimum values in the decision matrix, the Y_i value may be positive or negative in research. The ultimate preference of Y_i is displayed through an ordered ranking. As a result, the poorest alternative has the lowest Y_i value, and the greatest alternative has the highest Y_i value.

2.5. GRA and PCA

The integration of Grey Relational Analysis (GRA) with Principal Component Analysis (PCA) significantly enhances multi-optimization in welding processes [28]. This integration allows for the improvement of multiple quality responses, such as penetration, reinforcement, bead width, and dilution percentage, simultaneously. The weighted response analysis helps determine the relative importance of different quality responses, providing a more accurate representation of their impact on the overall optimization process [28]. This combination also allows for more informed decision-making regarding the selection of welding parameters, as PCA helps to classify the most significant parameters based on weighted responses. The integration of GRA and PCA has been proven to yield effective results in finding optimal combinations of welding parameters for multiple response optimizations, improving various quality responses in welding processes. This approach represents a novel and valuable contribution to the field, offering new insights and solutions for improving weld quality. Overall, the integration of GRA and PCA in welding optimization enables researchers to handle multiple responses, determine weighted influences of parameters, make informed decisions, achieve successful results, and contribute to the advancement of knowledge in the optimization of the welding process.

3. Results and Discussion

3.1. Probability plots

The experimental data distribution, as shown in ▶**Table 4**, is assessed using probability plots. The normality assumption is confirmed through Anderson-Darling test, a robust statistical method commonly used to detect outliers from a normal distribution [29]. ▶**Figure 3** shows that the data of all experiments and responses closely align with the fitted line, low Anderson-Darling statistics values, and a p-value greater than 0.05 [28], indicating that further analysis of the data is appropriate.

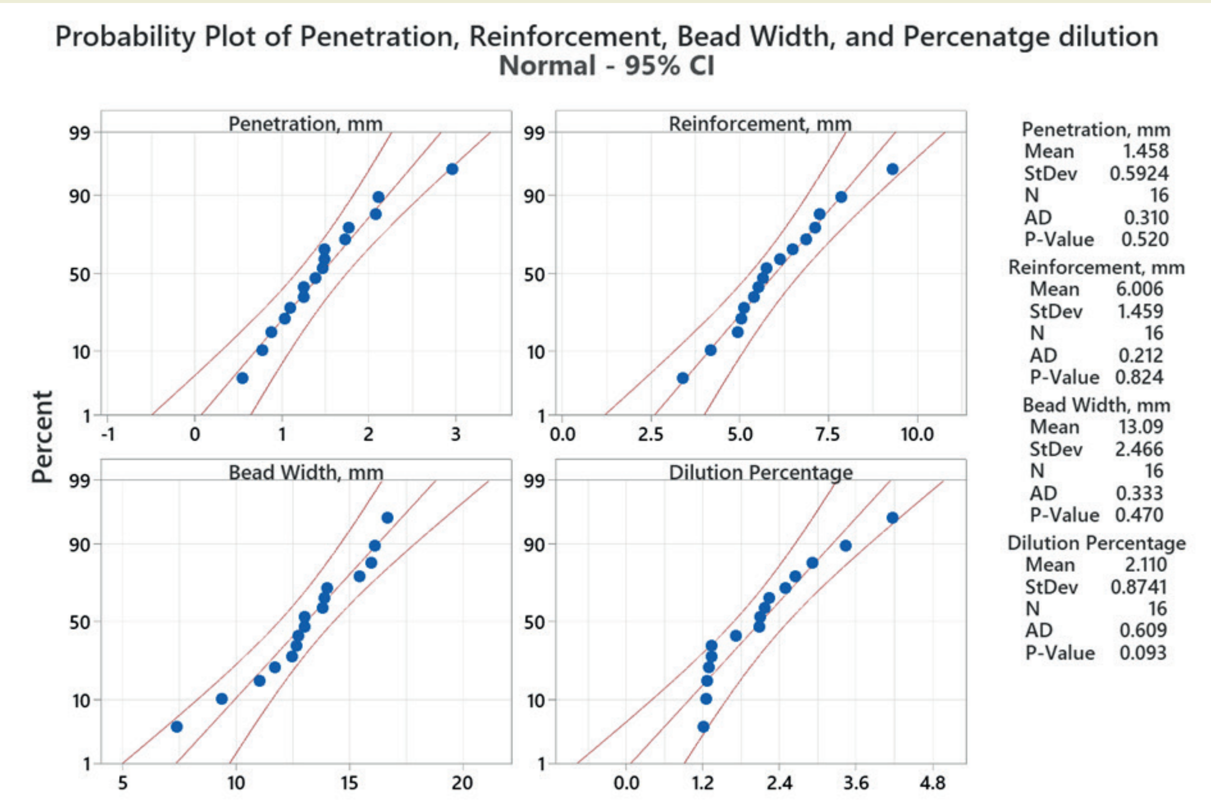

Figure 3. Probability plot for responses

3.2. Mean of Response

The influence of various welding parameters on the S/N ratio is individually examined as a result of the orthogonal design of the experiments. Graphs known as response curves illustrate how performance characteristics vary as input parameter levels change [10]. The graphs for response means are displayed in ▶Figures 4 to 7. Weld bead geometry quality attributes are influenced by process variables, as seen by the response graphs from the Taguchi experiment. Consequently, a thorough examination of how these factors affect the geometry of the weld bead is given in the sections that follow.

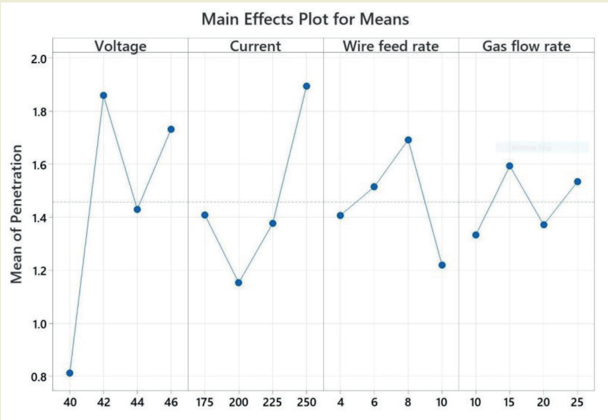

Figure 4. Main effect plots for mean of penetration

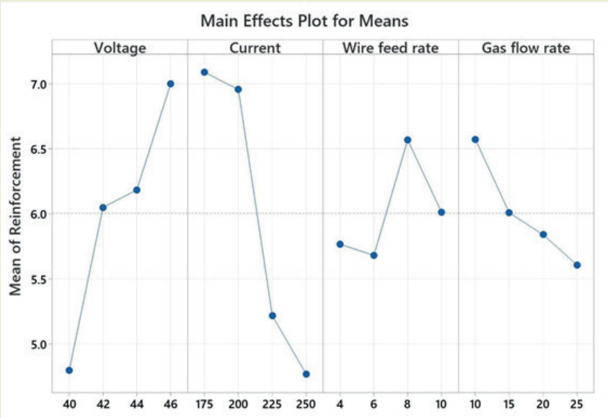

Figure 5. Main effect plots for mean of reinforcement

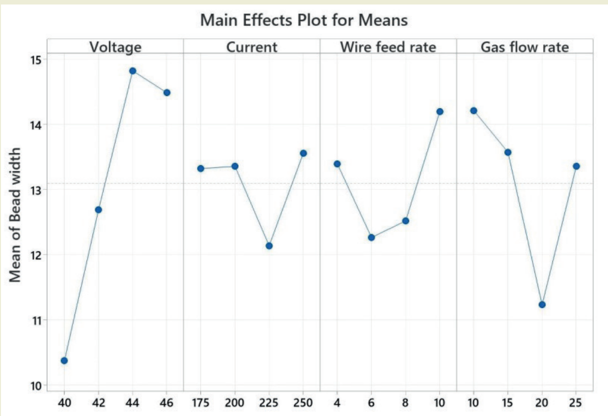

Figure 6. Main effect plots for mean of bead width

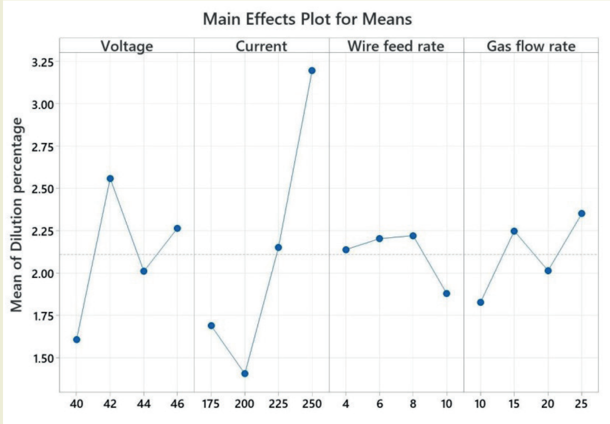

Figure 7. Main effect plots for mean of dilution percentage

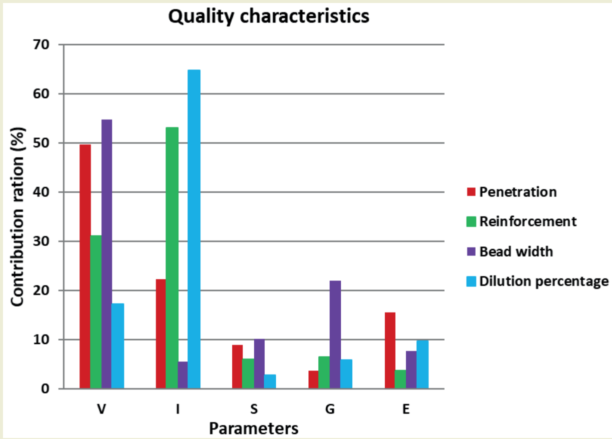

Figure 8. Pareto diagram for responses

3.3. ANOVA and contribution ratio

Table 5 provides the details of the calculation of the contribution ratio, which is derived from the total sum square of the difference. A method for identifying the significant process variables is Pareto analysis, which is also a quick and simple technique to analyze experiment findings [10]. The Pareto diagram's significant factors are chosen from the left side, where they collectively contribute 90%. It is clear from ▶Tables 5 and 6 that the depth of penetration and bead width is mostly determined by the Voltage. But out of all of these factors, welding current followed by voltage has the bigger impact on other parameters which include reinforcement, and dilution percentage. ▶Figure 8 displays the extracts of Pareto diagram.

4. MOORA

The weights of the variables are calculated and given in ▶Table 7. ▶Table 8 displays the normalized performance scores for various alternatives across specific attributes. These scores were determined using Equation (5). By applying Equation (7), the normalized values (Y_i) for every alternative were calculated based on these attributes. The table also presents the results of

MOORA method, organizing the alternatives in descending order of their assessment values. According to this method, experiment number 1 attained the top rank, following process parameters set at Voltage=40 V (level 1), Current=175 A (level 1), wire feed rate=4 mm/min (level 1), and gas flow rate 10 lpm (level 1).

5. Grey Rational Analysis

Maximizing reinforcement and bead width is of interest, depending on the aim of this article. Consequently, for these quality attributes, the larger-the-better criterion is chosen, and Equation (8) is used to express the normalized results.

$$y_j^*(q) = \frac{y_j(q) - min y_j(q)}{max y_j(q) - min y_j(q)} \tag{8}$$

It is also necessary to decrease penetration and dilution percentage, hence, as Equation (9) states, the smaller the better is used.

$$y_j^*(q) = \frac{max y_j(q) - y_j(q)}{max y_j(q) - min y_j(q)} \tag{9}$$

Where the generated grey relational values are denoted by $y_j^*(p)$, and the highest and lowest values of $y_j(q)$ for the q^{th} observation are represented by max $y_i(q)$ and min $y_i(q)$, respectively. The number of response variables is q = 4. The sixteen observations are listed in the comparable sequence $y_i(q)$, with j = 1, 2…,16. A greater value of normalized results is anticipated for improved performance, as the optimal normalized values equals 1.

After normalizing the data, Grey Relational Coefficients (GRC) are computed to demonstrate the correlation between the actual experimental outcomes and the desired ones. The expression for GRC $\xi_j(q)$ is provided in Equation (10).

$$\xi\left(y_j^*(q), y_0^*(q)\right) = \frac{\Delta_{min}(q) + \zeta\Delta_{max}(q)}{\Delta_{0j}(q) + \zeta\Delta_{max}(q)} \tag{10}$$

Where $|(q) + \zeta\Delta_{max}(q)|$ is the deviation sequence, defined as the absolute difference between reference sequence $y_0^*(q)$ and comparability sequence $y_j^*(q)$ [28]. The value of the identification or distinguishing coefficient (ξ) is between [0, 1], which in this paper was fixed at 0.5 [28]. Grey Relational Grade (GRG) is calculated from the weighted mean of the corresponding GRCs

Table 5. S/N response

Factors			V	I	S	G	Error	Total
Penetration	Sum at factor levels	1	2.042	-2.647	-2.545	-2.304		-10.403
		2	-4.903	-0.998	-3.067	-2.997		
		3	-2.981	-1.860	-3.155	-1.706		
		4	-4.562	-4.898	-1.636	-3.396		
	Sum of squares of differences		2.617	1.171	0.469	0.187	0.817	5.263
	Contribution ratio, %		49.724	22.250	8.911	3.553	15.523	100
Reinforcement	Sum at factor levels	1	13.370	16.990	15.170	16.100		61.310
		2	15.600	16.630	15.010	15.450		
		3	15.700	14.280	15.980	15.110		
		4	16.640	13.410	15.150	14.670		
	Sum of squares of differences		9.918	16.917	1.920	2.035	1.139	31.929
	Contribution ratio, %		31.063	52.983	6.013	6.374	3.567	100
Bead width	Sum at factor levels	1	20.120	22.380	22.490	22.970		88.700
		2	22.040	22.350	21.610	22.450		
		3	23.400	21.380	21.610	20.770		
		4	23.140	22.600	23.000	22.510		
	Sum of squares of differences		49.944	4.982	9.262	20.008	6.989	91.185
	Contribution ratio, %		54.772	5.464	10.157	21.942	7.665	100
Dilution percentage	Sum at factor levels	1	-3.600	-4.286	-5.974	-4.816		-23.343
		2	-7.640	-2.884	-6.482	-5.993		
		3	-5.800	-6.269	-5.856	-5.291		
		4	-6.303	-9.905	-5.031	-7.243		
	Sum of squares of differences		1.960	7.424	0.302	0.668	1.106	11.461
	Contribution ratio, %		17.101	64.776	2.635	5.828	9.650	100

https://doi.org/10.26701/ems.1621888

for each experimental run, which gives data about the strength of correlation among the welding runs. The GRG value ranges from 0 to 1. The ideal scenario is typically an experimental run with a greater GRG, which shows how strongly relevant experiments correlate with the idealized value. Equation (11) is used to calculate the GRG when all quality responses are given equal weights.

$$\gamma_j\left(y_0^*, y_j^*\right) = \frac{1}{n}\sum_{q=1}^{n} \xi\left(y_j^*(q), y_0^*(q)\right) \tag{11}$$

In certain practical uses, the weights of quality attributes vary similarly to the weights derived from PCA. Under these cases, Equation (11) undergoes a modification to become Equation (12) [28]:

$$\gamma_j\left(y_0^*, y_j^*\right) = \frac{1}{n}\sum_{q=1}^{n} Wq\, \xi\left(y_j^*(q), y_0^*(q)\right) \tag{12}$$

Where $\gamma_j\left(y_0^*, y_j^*\right)$ is GRG for jth experiment and n is the number of quality responses, Wq is the weight of qth quality response, and $\sum_{q=1}^{n} Wq = 1$

5.1. Principal Component Analysis

Principal Component Analysis is considered a reliable statistical method used to optimize several objectives simultaneously [28]. It simplifies and consolidates numerous related datasets into a few uncorrelated arrays and principal components, reducing complexity, correlation, vagueness, and dimensions of information [30]. A linear transformation is used in PCA to preserve as much distinctive information [31]. Therefore, PCA converts multi-response optimization to single-response optimization without varying the existing data [32]. It is achieved by constructing linear arrangements

Table 6. Results of ANOVA

Analysis of Variance for Penetration						
Source	DF	Adj SS	Adj MS	F-Value	P-Value	Rank
Voltage	3	2.617	0.87233	3.2	0.182	1
Current	3	1.1716	0.39055	1.43	0.387	2
Wire feed rate	3	0.4697	0.15658	0.57	0.67	3
Gas flow rate	3	0.1878	0.06259	0.23	0.871	4
Error	3	0.8172	0.27241			
Total	15	5.2634				
Analysis of Variance for reinforcement						
Source	DF	Adj SS	Adj MS	F-Value	P-Value	Rank
Voltage	3	9.918	3.3061	8.71	0.054	2
Current	3	16.917	5.6389	14.86	0.026	1
Wire feed rate	3	1.92	0.6401	1.69	0.339	4
Gas flow rate	3	2.035	0.6784	1.79	0.323	3
Error	3	1.139	0.3795			
Total	15	31.929				
Analysis of Variance for Bead width						
Source	DF	Adj SS	Adj MS	F-Value	P-Value	Rank
Voltage	3	49.944	16.648	7.15	0.07	1
Current	3	4.982	1.661	0.71	0.606	4
Wire feed rate	3	9.262	3.087	1.33	0.411	3
Gas flow rate	3	20.008	6.669	2.86	0.205	2
Error	3	6.989	2.33			
Total	15	91.185				
Analysis of Variance for Dilution percentage						
Source	DF	Adj SS	Adj MS	F-Value	P-Value	Rank
Voltage	3	1.9604	0.6535	1.77	0.325	2
Current	3	7.4238	2.4746	6.71	0.076	1
Wire feed rate	3	0.3021	0.1007	0.27	0.843	4
Gas flow rate	3	0.6679	0.2226	0.6	0.656	3
Error	3	1.1063	0.3688			
Total	15	11.4605				

Table 7. Weights of responses

Parameters	Penetration, mm	Reinforcement, mm	Bead Width, mm	Dilution Percentage
Weights	0.382	0.140	0.090	0.387

Table 8. Results of multi-criteria analysis and normalized decision-making matrix

Exp. no.	Weight Normalized matrix				ȳ	Rank
	Penetration	Reinforcement	Bead width	Dilution percentage		
1	0.054	0.037	0.020	0.318	-0.315	1
2	0.047	0.029	0.016	0.338	-0.340	4
3	0.033	0.024	0.012	0.328	-0.325	2
4	0.063	0.019	0.022	0.694	-0.716	13
5	0.106	0.039	0.019	0.546	-0.594	9
6	0.076	0.035	0.024	0.448	-0.466	7
7	0.091	0.031	0.022	0.586	-0.624	11
8	0.181	0.032	0.022	1.092	-1.219	16
9	0.108	0.041	0.023	0.549	-0.593	8
10	0.067	0.041	0.024	0.330	-0.332	3
11	0.084	0.031	0.026	0.568	-0.596	10
12	0.090	0.028	0.027	0.653	-0.687	12
13	0.076	0.045	0.028	0.351	-0.354	5
14	0.091	0.053	0.027	0.351	-0.362	6
15	0.127	0.033	0.021	0.765	-0.837	14
16	0.129	0.029	0.021	0.900	-0.978	15

for a variety of responses. The GRC (Generalized Reduced Coefficient) of the output variable is utilized for developing a matrix denoted by Equation (13).

$$y = \begin{bmatrix} y_1(1) & y_1(2) & \cdots & y_1(k) \\ y_2(1) & y_2(2) & \cdots & y_2(k) \\ \cdots & \ldots & \ldots & \ldots \\ \cdots & \ldots & \ldots & \ldots \\ y_j(1) & y_j(2) & \ldots & y_j(k) \end{bmatrix} \tag{13}$$

In this work, $y_a(q)$ denotes the GRC of an individual response, in which a is the total number of experiments (a = 1, 2, . . . j) and b is the total number of quality responses (b = 1, 2, . . . k). In this study, j is equal to 16, and k is equal to 4. Subsequently, the equation that follows can be utilized for creating the correlation coefficient matrix:

$$R_{jl} = \left(\frac{\mathrm{Cov}(y_a(b), y_a(l))}{\sigma_{ya}(b) * \sigma_{ya}(l)}\right) b = 1,2, \ldots k; l = 1,2, \ldots, k \tag{14}$$

The expression where Cov ($y_a(b)$, $y_a(l)$) represents the covariance among the sequences $y_a(b)$ and $y_a(l)$, while $\sigma_{ya}(b)$ and $\sigma_{ya}(l)$ represent the standard deviation of sequences $y_a(b)$ and $y_a(l)$, individually. The eigenvalues and eigenvectors were calculated from the R_{jl} array using Equation (15)

$$(R - \lambda_k I_j) V_{pk} = 0 \tag{15}$$

Consequently, Equation (16) is used to develop the uncorrelated principal components (PCs) from the eigenvalues (λ_k) and eigenvectors (V_{pk}) of the square matrix R

$$Z_{jk} = \sum_{i=1}^{n} Y_j(p) \times V_{pk} \tag{16}$$

In this equation, Z_{jk} refers to the k^{th} principal component. The initial eigenvalue related to the first principal component (PC) explains the major contribution of variance, where the eigenvalues and principal components are organized in descending order based on their described variance. ▶**Table 9** presents the eigenvalues associated with the eigenvectors.

Table 9. Principal Component Analysis

Component	PC1	PC2	PC3	PC4
Eigenvalue	1.9199	1.5786	0.4939	0.0076
Variation (%)	0.48	0.395	0.123	0.002
Cumulative (%)	0.48	0.875	0.998	1
Eigen Vector	0.688	0.118	-0.363	0.617
	-0.082	0.723	-0.57	-0.382
	0.208	0.642	0.734	0.077
	0.69	-0.225	0.073	-0.684

 https://doi.org/10.26701/ems.1621888

5.2. Optimization of multiple variables by utilizing GRA and PCA

Because every response variable in GRA has identical weights, choosing decisions may be difficult. Thus, PCA has been utilized for determining the relative weights of quality responses [33]. This study compares the multi-objective optimization processes carried out by PCA and GRA. The section on optimization methodology goes into comprehensive detail on the steps. Equations (8) and (9) are first used to normalize the S/N ratios. Equation (10) is utilized to calculate the Grey relationship coefficient of individual response. ▶Table 9 displays the Eigen values and Eigen vectors for PCA, which were computed using Equation (15) and PC from Equation (16). The Eigenvectors of the first PC are squared to yield relative weights of the quality responses. Using the weights determined by PCA and GRCs that are listed in ▶Table 9 are computed for sixteen experiments using Equation (11).

Sample number eight yields the maximum GRG value. ▶Table 10 makes it clear that the first PC contributes up to 47.33% of the variance for four quality attributes. The squares of the eigenvectors of the first PC, which are selected as weights of quality responses, are shown in ▶Table 10 and are determined to be, in the order of penetration, reinforcement, bead width, and dilution percentage of 0.4733, 0.0067, 0.0433, and 0.4761 respectively. Thus, with regard to individual GRG, the ideal multi-objective optimization can be accomplished. Hence, from GRG, $A_2B_4C_3$ that is, Voltage=42 V (level 2), Current=250 A (level 4), wire feed rate=8 mm/min (level 3), and gas flow rate 15 lpm (level 2) represents the ideal collection of input parameter values for optimum responses.

6. Conclusion

The SN ratio is used to identify interactions among input and process parameters. MOORA method ranks parameters based on calculated weights while GRA with PCA assigns equal weights to all parameters to determine the optimized parameters. This study compares these methods, enabling industries to select the suitable optimization process from the available methods based on their specific requirements. The results contributed to reducing the welding defect in the small-scale industry where the experiments were conducted. By reducing the number of experiments and associated costs, it is possible to identify optimized solutions for the existing welding machines and the given job.

- Using S/N ratio for single objective optimization concludes that:
- For reduced penetration, V=42 V, I=250 A, S=8 mm/min, and G=15 lpm
- For enlarged reinforcement, V=46 V, I=200 A, S=8 mm/min, and G=10 lpm
- For enlarged bead width, V=46 V, I=175 A, S=10 mm/min, and G=15 lpm
- For reduced dilution percentage, V=42 V, I=250 A, S=8 mm/min, and G=15 lpm.
- Predominantly voltage affects penetration and bead width whereas welding current affects reinforcement and dilution percentage.
- Through the MOORA method, it was determined

Table 9. Calculated Normalized GRC, and GRG for 16 experiments

Exp. No.	Normalization				Grey Relational Coefficient				GRG	Rank
1	0.283	0.641	0.567	0.000	0.411	0.582	0.536	0.333	0.466	14
2	0.205	0.405	0.295	0.048	0.386	0.456	0.415	0.344	0.401	15
3	0.000	0.202	0.000	0.024	0.333	0.385	0.333	0.339	0.348	16
4	0.380	0.000	0.697	0.633	0.446	0.333	0.623	0.577	0.495	13
5	0.682	0.699	0.496	0.439	0.612	0.624	0.498	0.471	0.551	9
6	0.489	0.584	0.777	0.278	0.494	0.546	0.691	0.409	0.535	12
7	0.593	0.482	0.699	0.496	0.551	0.491	0.624	0.498	0.541	11
8	1.000	0.505	0.671	1.000	1.000	0.502	0.603	1.000	0.776	1
9	0.694	0.733	0.771	0.443	0.620	0.652	0.685	0.473	0.608	7
10	0.411	0.752	0.787	0.031	0.459	0.668	0.702	0.340	0.542	10
11	0.550	0.458	0.908	0.470	0.526	0.480	0.844	0.485	0.584	8
12	0.585	0.373	0.946	0.582	0.546	0.444	0.902	0.545	0.609	6
13	0.489	0.831	1.000	0.080	0.494	0.747	1.000	0.352	0.648	3
14	0.593	1.000	0.958	0.080	0.551	1.000	0.922	0.352	0.706	2
15	0.791	0.524	0.662	0.711	0.705	0.512	0.597	0.634	0.612	5
16	0.799	0.391	0.645	0.843	0.713	0.451	0.584	0.761	0.627	4

Table 10. Variance contribution of response variables for first PC

Response Variable	Contribution
Penetration	0.4733
Reinforcement	0.0067
Bead width	0.0433
Dilution percentage	0.4761

that a voltage of 40V, welding current of 175A, wire feed rate of 4 mm/min, and gas flow rate of 10 lpm would yield optimal weld bead geometry with penetration of 0.884 mm, reinforcement of 6.489 mm, bead width of 11.715 mm, and dilution percentage of 1.218%.

- From PCA and GRA, setting the voltage at 42V, welding current at 250A, wire feed rate at 8 mm/min, and gas flow rate at 15 lpm results in ideal characteristics: penetration of 2.961 mm, reinforcement of 5.658 mm, bead width of 12.753 mm, and dilution percentage of 4.183%.

Research ethics

Not applicable.

Author contributions

Methodology – Raviram R, Ranjith Raj A; Formal Analysis – Raviram R, Shashang G, Shameer Mohamed S; Investigation – Raviram R, Shashang G; Resources – Raviram R, Ranjith Raj A; Data Curation – Raviram R; Writing – Original Draft Preparation – Raviram R; Writing – Review & Editing – Raviram R, Ranjith Raj A; Visualization – Raviram R, Shashang G, Shameer Mohamed S; Supervision – Ranjith Raj A; Project Administration – Raviram R, Ranjith Raj A; Funding Acquisition – Raviram R.

Competing interests

The author state(s) no conflict of interest.

Research funding

None declared.

Data availability

Not applicable.

Peer-review

Externally peer-reviewed.

Orcid

Raviram R https://orcid.org/0009-0005-5837-1239
Ranjith Raj A https://orcid.org/0000-0003-3125-8146
Shashang G https://orcid.org/0009-0007-9673-1674
Shameer Mohamed S https://orcid.org/0009-0005-7444-9657

References

[1] Baskoro, A. S., Hidayat, R., Widyianto, A., Amat, M. A., & Putra, D. U. (2020). Optimization of Gas Metal Arc Welding (GMAW) Parameters for Minimum Distortion of T Welded Joints of A36 Mild Steel by Taguchi Method. Materials Science and Engineering, 1000, 356–363. doi: 10.4028/www.scientific.net/msf.1000.356

[2] Ramarao, M., King, M. F., Sivakumar, A., Manikandan, V., Vijayakumar, M., & Subbiah, R. (2022). Optimizing GMAW parameters to achieve high impact strength of the dissimilar weld joints using Taguchi approach. Materials Today: Proceedings, 50, 861–866.

[3] Adin, M. Ş., & İşcan, B. (2022). Optimization of process parameters of medium carbon steel joints joined by MIG welding using Taguchi method. European Mechanical Science, 6(1), 17–26.

[4] Madavi, K. R., Jogi, B. F., & Lohar, G. S. (2022). Metal inert gas (MIG) welding process: A study of effect of welding parameters. Materials Today: Proceedings, 51, 690–698.

[5] Titinan, M., Masaya, S., Manabu, T., Rinsei, I., Muneo, M., & Tokihiko, K. (2017). Diagnostic of heat source characteristics in gas metal arc welding using CO2 shielding gas. 溶接学会論文集, 35(2), 103s–107s.

[6] Narwadkar, A., & Bhosle, S. (2016). Optimization of MIG welding parameters to control the angular distortion in Fe410WA steel. Materials and Manufacturing Processes, 31(16), 2158–2164.

[7] Sankar, B. V., Lawrence, I. D., & Jayabal, S. (2018). Experimental study and analysis of weld parameters by GRA on MIG welding. Materials Today: Proceedings, 5(6), 14309–14316.

[8] Pal, A. (2015). MIG welding parametric optimisation using Taguchi's orthogonal array and analysis of variance. International Journal of Research Review in Engineering Science and Technology, 4(1), 211–217.

[9] Kumar, P., & Roy, B. K. (2013). Parameters Optimization for Gas Metal Arc Welding of Austenitic Stainless Steel (AISI 304) & Low Carbon Steel using Taguchi's Technique. International Journal of Engineering and Management Research, 3(4), 18–22.

[10] Palani, P. K., Murugan, N., & Karthikeyan, B. (2006). Process parameter selection for optimising weld bead geometry in stainless steel cladding using Taguchi's approach. Materials Science and Technology, 22(10), 1193–1200.

[11] Montgomery, D. C. (2006). Design and analysis of experiments (4. baskı). New York: John Wiley & Sons.

[12] Ross, P. J. (1988). Taguchi techniques for quality engineering. New York: Tata McGraw Hill.

[13] Park, S. H. (1996). Robust design and analysis for quality engineering (1. baskı). Londra: Chapman & Hall.

[14] Ross, P. J. (1996). Taguchi techniques for quality engineering. New York: McGraw-Hill.

[15] Belavendran, N. (1995). Quality by design. Londra: Prentice Hall.

[16] Yang, W. H., & Tarng, Y. S. (1998). Design optimization of cutting parameters for turning operations based on the Taguchi method. Journal of Materials Processing Technology, 84, 122–129.

[17] Songa, Y. A., Parka, S., & Chaeb, S. W. (2005). Optimization of the injection molding process for part warpage using Taguchi method.

International Journal of Machine Tools & Manufacture, 45(1), 1–7.

[18] Syrcos, G. P. (2003). Die casting process optimization using Taguchi methods. Journal of Materials Processing Technology, 135, 68–74.

[19] Gadakh, V. S., Shinde, V. B., & Khemnar, N. S. (2013). Optimization of welding process parameters using MOORA method. The International Journal of Advanced Manufacturing Technology, 69, 2031–2039.

[20] Brauers, W. K. M. (2004). Optimization methods for a stakeholder society: A revolution in economic thinking by multiobjective optimization. Boston: Kluwer Academic.

[21] Brauers, W. K. M., Zavadskas, E. K., Peldschus, F., & Turskis, Z. (2008). Multi-objective decision-making for road design. Transport, 23, 183–193.

[22] Brauers, W. K. M., Zavadskas, E. K., Peldschus, F., & Turskis, Z. (2008). Multi-objective optimization of road design alternatives with an application of the MOORA method. Proceedings of the 25th International Symposium on Automation and Robotics in Construction, Lithuania, 541–548.

[23] Brauers, W. K. M. (2008). Multi-objective contractor's ranking by applying the MOORA method. Journal of Business Economics and Management, 4, 245–255.

[24] Brauers, W. K. M., & Zavadskas, E. K. (2009). Robustness of the multiobjective MOORA method with a test for the facilities sector. Technological and Economic Development of Economy, 15(2), 352–375.

[25] Kalibatas, D., & Turskis, Z. (2008). Multicriteria evaluation of inner climate by using MOORA method. Information Technology and Control, 37, 79–83.

[26] Brauers, W. K. M., & Zavadskas, E. K. (2010). Project management by MULTIMOORA as an instrument for transition economies. Technological and Economic Development of Economy, 16(1), 5–24.

[27] Lootsma, F. A. (1999). Multi-criteria decision analysis via ratio and difference judgement. Londra: Springer.

[28] Qazi, M. I., Akhtar, R., Abas, M., Khalid, Q. S., Babar, A. R., & Pruncu, C. I. (2020). An integrated approach of GRA coupled with principal component analysis for multi-optimization of shielded metal arc welding (SMAW) process. Materials, 13(16), 3457.

[29] Stephens, M. A. (1974). EDF statistics for goodness of fit and some comparisons. Journal of the American Statistical Association, 69, 730–737.

[30] Seong, W.-J. (2019). Prediction and characteristics of angular distortion in multi-layer butt welding. Materials, 12, 1435.

[31] Armentani, E., Esposito, R., & Sepe, R. (2007). The influence of thermal properties and preheating on residual stresses in welding. International Journal of Computational Materials Science and Surface Engineering, 1, 146–162.

[32] Ramasamy, N., Jeyasimman, D., Kathiravan, R., & Raju, N. (2019). Influence of Welding Sequence on Residual Stresses Induced in As-Welded Plug Weld of Low-Carbon Steel Plate. Transactions of the Indian Institute of Metals, 72, 1361–1369.

[33] Chate, G. R., Patel, G. M., Kulkarni, R. M., Vernekar, P., Deshpande, A. S., & Parappagoudar, M. B. (2018). Study of the effect of nano-silica particles on resin-bonded moulding sand properties and quality of casting. Silicon, 10, 1921–1936.